Fatigue in Aircraft Structures
Vol. 1 (2009) 170-190
10.2478/v10164-010-0015-9

EXPERIMENTAL AND THEORETICAL INVESTIGATIONS OF FATIGUE CRACK GROWTH IN D16 ALLOY

Lucjan Śnieżek

Military University of Technology
Warsaw, Poland

Abstract

In this work the arising and development of fatigue crack in aluminium alloy D16, taking into consideration the influence of notch in the form of hole with incisions which were done on its sides were tested. The process of working out of tests' programme was preceded by numeric analysis of stresses pattern and strains distribution in the zone of notch's influence which was focused on determination of stresses' face values. To examine stress and strain distributions, the specialised FEM software (MSC.Patran and MSC.Nastran) was applied. Findings have been presented in the form of a statement of σ_{max} and ε_{max} values, and functions of the following factors: a_σ, a_ε, and a_k, computed on the grounds of these values for both different distances from the bottom of the notch and assumed levels of loading the specimens. Theoretical analysis has been supplemented with experimental investigation into the microstructure of fatigue-fracture surfaces in the area of crack initiation and that of fatigue of a propagating crack. The paper has been intended to present a model of the probabilistic estimation of fatigue life of structural members. The model has been based on the deterministic description of the cracking. Analyzed were components with notches in the form of centrally located holes with side cuts. In the method of probabilistically approaching the crack propagation, some dependences have been used that take account of the presence of areas showing plastic strains in front of crack tips. It has been assumed that the cracking can be modeled on the grounds of some general-purpose quantity used to describe the energy state in the area of the crack tip, i.e. the Rice's integral (J). The formulated computational model has been used to estimate fatigue life of model components made of D16 alloy. Experimental work was carried out using some flat specimens with centrally positioned holes. They were exposed to flat bending at R = 0. Analytical and experimental results have shown pretty good conformity.

1. INTRODUCTION

Fatigue crack propagation and fatigue life are issues of great significance to structural components and their getting failed/damaged, not yet thoroughly recognized. The deepest knowledge possible in this field proves of vital importance because of serious effects of any potential failure/damage (aircraft, chemical pipelines, water-supply systems in nuclear power plants, etc.). Identifying the characteristic features of the development of fatigue cracks in materials used in aeronautical industry is of great importance, especially with reference to aircraft skins. It is connected with the possibility of servicing aeronautical structures under the conditions of the presence of cracks that either do not propagate or grow at a low rate. Using aluminium alloys in aircraft skins is connected with the necessity of investigating the fatigue behaviour of the materials, with taking into consideration the effects of different factors on their fatigue cracking. Any analysis of phenomena, which occur where geometric and structural discontinuities (generally called 'notches') are found, proves more difficult especially in instances of loads producing low-cycle fatigue. Stress concentration at the bottom of a notch often provokes some plastic strain of

the material in this area, which - in case of cyclic loads – results in both origination of internal stresses and change in the mean stress. For many years, the effects of some local yielding-inducing stress concentrations upon fatigue behaviour of materials and structural components have been studied in numerous scientific centres world-wide [1-4]. It is extremely difficult to take account of this phenomenon in strength computations, especially while using analytical solutions expected to comprise its 3D nature, a complicated shape of the notch, and the effect of boundary conditions. Determination of actual stress and strain levels in the region of fatigue crack initiation would considerably facilitate interpretation of phenomena that go together with the process, and often affords any description of fatigue cracking of tested members with stress concentrators in the form of suitably cut crack initiator [5-8]. Application of a numerical method offers a chance to find some approximate solution to the above-described problem, however, with some limitations. Among various available methods, the finite element method (FEM) is the most common technique suitable to solve the problem given consideration. Professional software proves of great assistance while solving problems with this method. However, good knowledge of the FEM theory and some experience in computer modelling are needed. Evaluation of fatigue strength and resistance to cracking is probably the most fundamental criterion, one of decisive role in applying some selected alloys in structures of constructions (e.g. aircraft). Along with the progress in designing/developing high-risk structures, modified design methods are introduced, e.g. safe-life and fail-safe concepts, and new materials-production technologies. They are based on new materials characteristics which include, among other ones, an extended approach to mechanisms underlying both the crack propagation and the effect of the notch dimensions upon crack propagation rate, i.e. factors expected to ensure the required fatigue life of the structure of a given construction. Apart from investigating into mechanical properties of these materials, recent years have been featured with much more intense efforts that take account of a notch in a structural member under examination [9-10].

The fatigue crack propagation depends on many and various factors, stochastic in their nature, e.g. how the loading has proceeded, the component's geometry, properties of the material, etc. Therefore, the application of probabilistic models of crack propagation seems strongly advisable. This approach to the problem of fatigue life is represented, among others, by the Authors of [11-14]. Determination of the component's life, from the probabilistic standpoint, needs knowledge of the service-induced cracking, including a complete probabilistic description of crack propagation, with information on stochastic factors of the cracking included. Hence, the probabilistic model assumed should both take account of fundamental dependences that describe the cracking dynamics, and be based on the experimental findings.

The present paper discusses the research on the development of fatigue cracks in the D16 alloy under the conditions of the presence of a geometric notch in the form of a central hole with side cuts. The paper has been intended to present a model making use of a difference equation that describes the crack growth dynamics approached probabilistically. This approach has been suggested by H. Tomaszek, and discussed in more details in, e.g. [15-16]. For the instance of cracking given consideration, a differential equation has been introduced, which takes account of the dependences specific to a deterministic model. The Gaussian probability distribution of crack lengths offers a solution to this equation. Outlined is the way of estimating the needed coefficients, with the well-known methods (the maximum likelihood method, the least squares method, and that of bisection) described in the literature of the subject – neglected. With some probability distribution that includes known parameters and for the assumed risk of exceeding the acceptable crack-length limit, fatigue life of a given component has been estimated.

Analytical considerations have been supported with exemplary computations based on experimental findings from tests of model members.

2. MATERIAL, SPECIMENS AND RESEARCH METHODOLOGY

The D16 aluminum alloy (2.85% Cu, 2.18% Mg, 0.38% Mn, 1.40% Si, 0.18% Ti, 0.28% Fe) of Russian production was used in the research. The material was delivered in the form of 3-mm-thick cold-rolled sheets. The microstructure of the alloy being examined is presented in metallographic images in Figure 1. In the images, there are noticeable flat grains (the rolling texture) placed one on another in the sheet plane. The alloy is characterized by a fine-grained structure with precipitates abounding in copper and ferrum. Grain size is of the order of 15 ÷ 30 μm (see Fig. 1a), whereas the plate width is about 90 ÷ 100μm (see Fig. 1b)

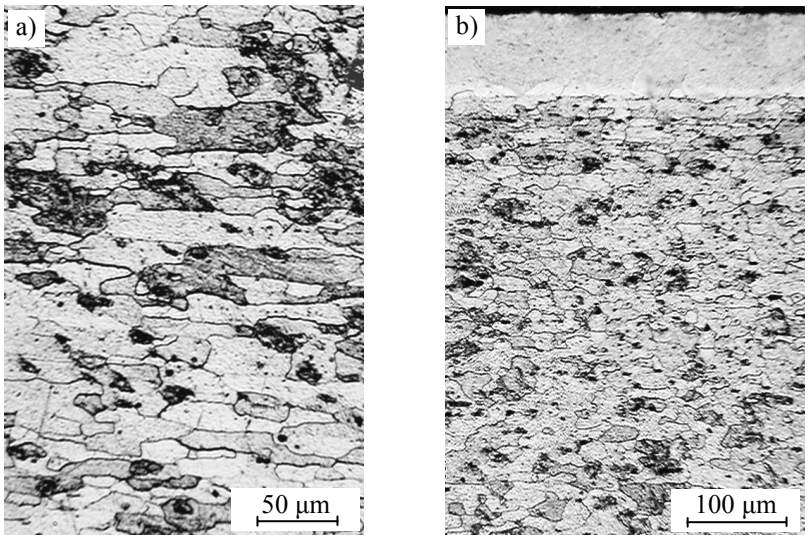

Fig. 1. The microstructure of the D16 alloy longitudinal (a) and at the angle of 90° (b) to the rolling direction.

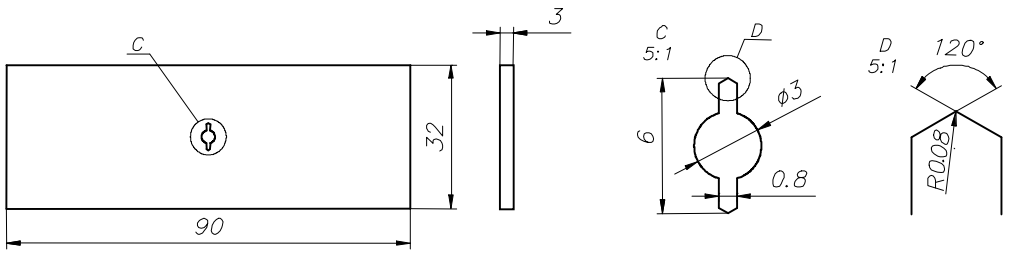

Fig. 2. Dimensions of specimens

Flat specimens of dimensions shown in Fig. 2 were used in the essential testing work. They were cut out in the direction of sheet rolling. Slots were cut out in the form of centrally located holes of 3 mm diameters with side cuts of total length of 6 mm (see Detail C in Fig. 1). These were crack initiators. The outlines of cut tips and the radius of the notch bottom are illustrated with Detail D. The size of the radius of the notch bottom, R = 0.08 mm, was reached using a suitably profiled hook tool. The contour of the cuts made in the specimens of the alloy being examined is shown in Fig. 3.

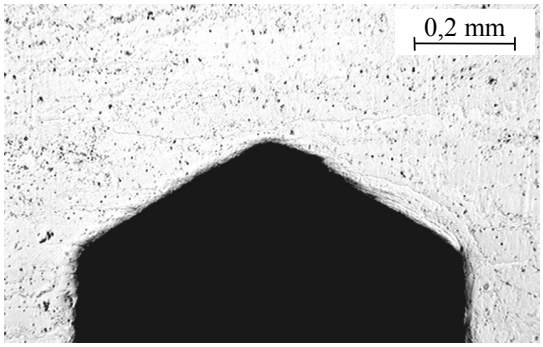

Fig. 3. The contour of initial fissures.

The metallographic research was conducted with the use of a NEOPHOT 2 microscope. In order to prepare metallographic microsections, specimens were polished and then anodized. Static mechanical properties were assessed in a fatigue strength test performed by means of an INSTRON 8802 hydraulic pulsator with an INSTRON 2630-112 type extensometer. The analysis of the chemical composition of the alloys was carried out by means of an EDAX chemical composition microanalyzer. In order to analyze the distribution of stresses and deformations in notch-affected zone, the FEM (MSC Patran and MSC Nastran) software was used. Fatigue crack growth tests were conducted under the conditions of alternating bending at the frequency of load changes of 25 Hz. Crack lengths of specimen surfaces were recorded with the use of acetylcellulose replicas, crack propagation gages as well as by means of the optical method with the use of a NEOPHOT 2 light microscope with a digital image analyzer LUCIA. Each time the testing machine was stopped, specimens were taken out and replicas were placed on the measurement area, moreover, measurements were taken on the screen of the image analyzer.

The fatigue crack propagation mechanism was scrutinized in terms of examining the microstructure of fracture surfaces by means of a TEM JEOL JEM 1230 microscope with the use of acetylcellulose replicas dusted with carbon and shaded with platinum.

3. A NUMERICAL ANALYSIS OF THE DISTRIBUTION OF STRESSES AND DEFORMATIONS

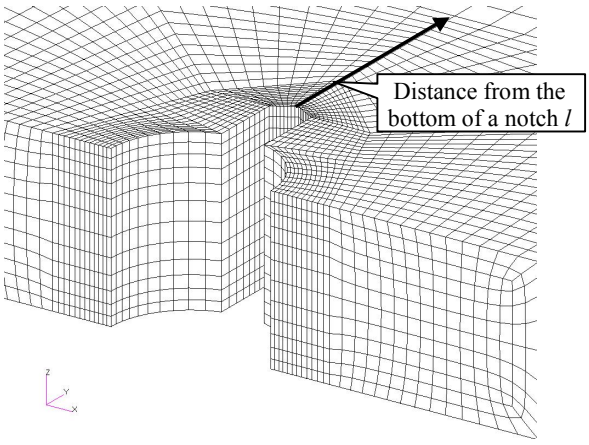

Fig. 4. A discrete FEM model assumed for analysis

To investigate into stress and strain distributions, the highly specialised FEM software (MSC.Patran and MSC.Nastran) was used. In the first step, a geometric model of a half-specimen was made, with a notch being a crack initiator well represented. In the next step, the mesh model found was created by means of the Hex elements. The total number of elements used was 35456 (Fig. 4).

The FEM mesh was compacted around the notches where strong stress concentration is generated. The in the calculations assumed boundary conditions resulted from the symmetry of the specimens, conditions of fitting them on the test station, and the performed loading which was producing the bending effect – at one end the test bar was subjected to bending by force, whereas at the opposite end it was fixed.

The next step in the algorithm of numerical calculations was to introduce material properties of the structure under analysis. A complete characteristics in the form of a curve $\sigma = f(\varepsilon)$ was used in the calculations. The Huber-Mises condition was assumed a criterion of the plastic yielding of the material. While performing computations with the MSC/Nastran, the basic system of differential equations was applied, one that described the equilibrium of a loaded elastic-plastic body. The tangential matrix present in the matrix equation of equilibrium is the so-called elastic-plastic matrix, which results from the incremental form of the constitutive law.

The finite element method (FEM) offers procedures that facilitate solving non-linear problems. They can be grouped into three classes: incremental (step-by-step), iterative (*Newton-Raphson's, Broylen-Fletcher-Goldfarb-Shanno* – BFGS), and mixed (incremental/ iterative, step-by-step/iterative) procedures. In the calculations made, the method quickly convergent in respect of the number of iterations was used, i.e. the *Newton-Raphson's* method. However, in each iteration a new tangential matrix of stiffness is created, which extends time needed for computations.

Values of the amplitude of nominal bending stresses σ_{bna} assumed for the needs of analysis result from the range of specimen loading, assumed in the experimental work. The tests were carried out under flat-bending conditions, at the amplitude of nominal bending stresses σ_{bna} = 80, 90, 100 and the stress ratio R = -1.

The conducted numerical analysis has facilitated solving the problem of stress and strain concentrations around notches. Fig. 5 show some selected computational results in the form of maps of reduced stresses and plastic strains in the areas of notches made in the specimens, at the amplitude of nominal bending stresses σ_{bna} = 100 MPa. For different values of σ_{bna} and with these maps employed, plotted were curves of total strains ε_c depending on the distance l from the bottom of the notch cut out in the direction shown in Fig. 4 (Fig. 6).

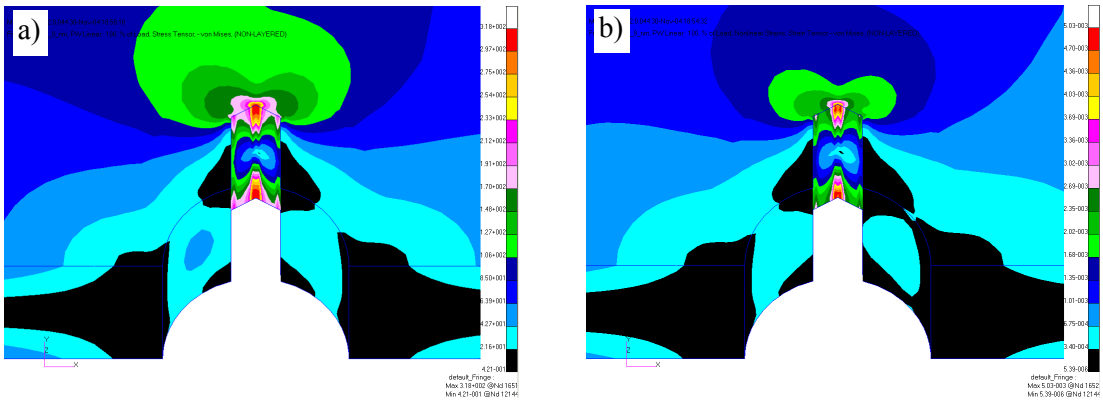

Fig. 5. Distributions of: (a) reduced stresses, and (b) plastic strains in the notch-affected area in a specimen of the D16 alloy, examined at σ_{bna} = 100 MPa

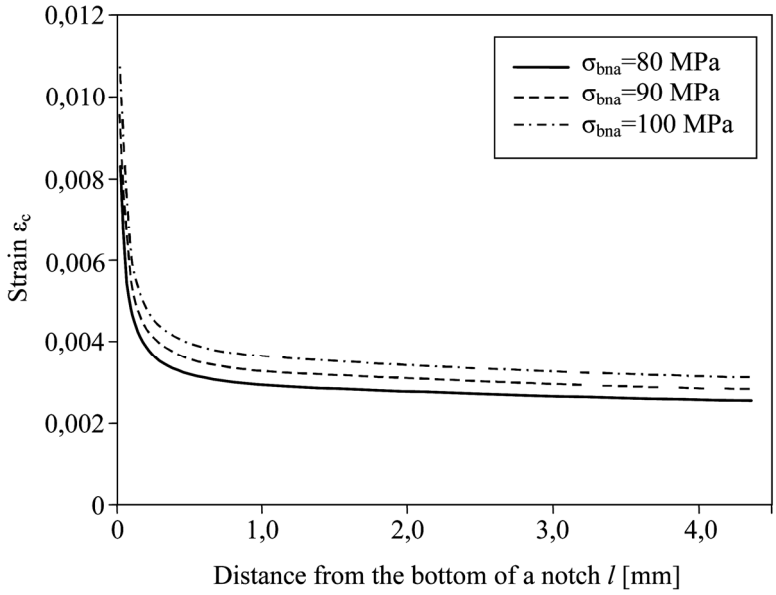

Fig. 6. Distribution of total strain $\varepsilon_c = f(l)$ in components made of the D16 alloy

Results of computations of the amplitude of the actual bending stress σ_{ba} and the corresponding total strain ε_c depending on the distance l from the notch, for different values of the amplitude of the nominal bending stress σ_{bna} are presented in Fig. 7.

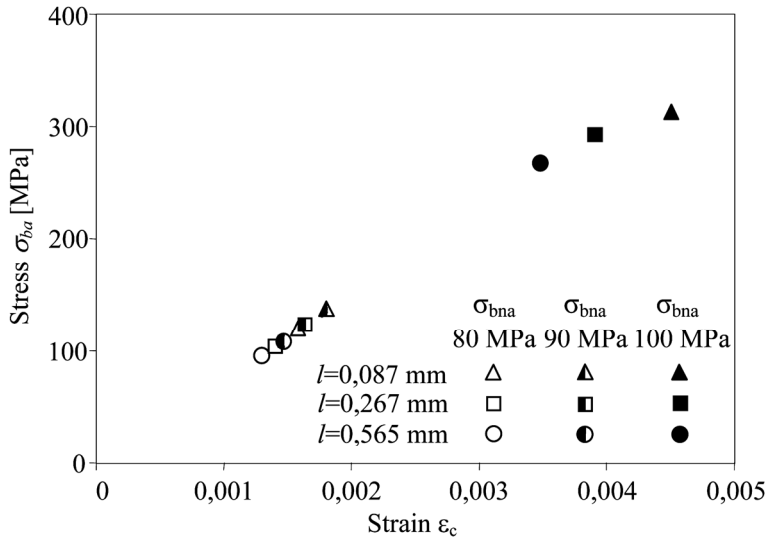

Fig. 7. Results of calculations gained for stress σ_{ga} and strain ε_c in components made of the D16 alloy

The observed stress and strain concentrations, α_σ and α_ε - respectively, are localised and rapidly decrease as the distance from the bottom of the notch increases. The intensity of these concentrations can be determined using a shape factor α_k, which – according to the H. Neuber's concept – is a geometric mean of factors α_σ and α_ε:

$$\alpha_k^2 = \alpha_\sigma \cdot \alpha_\varepsilon \tag{1}$$

with $\alpha_\sigma = \dfrac{\sigma_{\max}}{\sigma_n}$, and $\alpha_\varepsilon = \dfrac{\varepsilon_{\max}}{\varepsilon_n}$.

In the expressions above, σ_{max} and ε_{max} are maximum values of local stresses and strains, and σ_n and ε_n are nominal values thereof. The statement of values of σ_{max} and ε_{max}, found with the finite element method, and factors α_σ, α_ε, and α_k calculated on the grounds of these values, for notches cut out in specimens are presented in Tab. 1.

Table 1. Values of σ_{max} and ε_{max}, and factors α_σ, α_ε, and α_k for notches made in specimens fabricated of the D16 alloy

σ_{bna}[MPa]	ε_n	σ_{max} [MPa]	ε_{max}	α_σ	α_ε	α_k
80	0,0026	410	0,0083	5,125	3,192	4,045
90	0,0029	440	0,0095	4,889	3,276	4,002
100	0,0032	460	0,0108	4,600	3,375	3,940

As the loading increases, values of α_σ, α_ε, and consequently, α_k, change in the way shown in Figs 9 and 10. Nominal stresses accepted in the course of analysing the D16 alloy, i.e. σ_{bna} = 80 - 100 MPa, provoked considerable stress concentration in the area of the notch tip. This stress concentration was greater (for the whole range of applied loads) than the strain concentration. This affected the value of the shape factor calculated for the specimens made of this alloy, i.e. α_k = 3.940 - 4.045. Results of calculations confirmed the argument that plastic flow of the material limits value of the stress concentration factor α_σ, which cannot be stated about the strain concentration factor α_ε. The plastic flow of the material considerably increases the maximum local strain, and consequently, α_ε. Therefore, under conditions featured with macroscopic plastic strains, the level of α_ε can prove of greater significance than that of α_σ.

4. EXPERIMENTAL RESEARCH ON THE PROPAGATION OF FATIGUE CRACKS

Crack growth in real metallic materials is closely connected with the plastic strain zone ahead of the crack front and, therefore, restricts the application of the rules of classic cracking mechanics. In that case, the J-integral appears to be more universal for describing the stress field, or to be more precise, the energy state in the precrack front zone. As it applies to the elastic-plastic range, it is also suitable for describing crack growth rates under the conditions of the presence of plastic strains. The J-integral range, ΔJ, has been used for expressing crack growth since the beginning of the 1980s. In describing crack growth rates, one oftentimes comes across the expression (2):

$$\frac{dl}{dN} = C(\Delta J)^m \tag{2}$$

where C and m are material constants, whereas ΔJ is the J-integral range.

The value of ΔJ may by determined from the formula (3), which was proposed by Dowling in reference [17].

$$J_{max} = \left[1{,}24\frac{(\sigma_{max})^2}{E} + 1{,}02\frac{\sigma_{max}\varepsilon_{max}}{\sqrt{n'}}\right] l \tag{3}$$

where: J_{max} – max value of J integral,
E – Young's modulus,
σ_{max} – max stress,
ε_{max} – max strain,
n' – coefficient of cyclic strain-hardening,
l – actual length of the crack.

The expression (3) and the results of measurements concerning the fatigue crack length increment were used for producing the diagrams of crack propagation and fatigue crack growth rates of the analyzed model components made of the D16 alloy.

4.1. Fatigue crack growth

Fatigue crack growth tests were conducted at three levels of nominal bending stresses, namely σ_{bna} = 80, 90 and 100 MPa. The selection of stress values was made on the basis of the results of static strength properties tests and the numerical analysis of the distribution of stresses and deformations in the vicinity of the initial fissure tip. Crack lengths on specimen surfaces were measured with the use of acetylcellulose replicas and by recording images by means of a NEOPHOT 2 light microscope with a digital image analyzer, LUCIA. *Crack propagation gages* were used in order to verify the measurements. The results of crack length measurements made with the use of replicas and crack propagation gages with the *measuring base of* 0.25 mm were compared. The results of the comparison were satisfactory. Test results are illustrated in the diagrams of stress changes in the function of the number of cycles to failure, U=f(N), as well as crack length in the function of the number of cycles to failure, l=f(N), which were produced for the analyzed specimens (see Fig. 8).

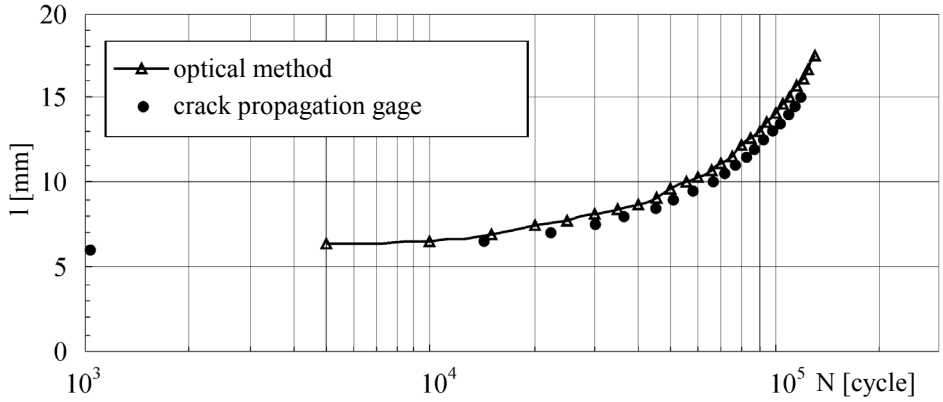

Fig. 8. The diagram of crack length changes in the function of the number of cycles to failure l=f(N) for a D16 alloy specimen tested at σ_{bna}=80 MPa

The results of the measurements of crack lengths, l, for a specific number of cycles, N, constituted the basis for producing l=f(N) and l = f(N_i/N_f) diagrams (see Fig. 9a, 9b), where N_i is the number of current cycles, whereas N_f is the number of cycles to failure.

The processes of the emergence and development of cracks in the two analyzed alloys were very similar. In all tested specimens, crack initiation took place at the notch bottom in slip bands located in the matrix of the tested alloy. The nature of crack initiation is determined by phenomena connected with the dislocation appearance process. It is conductive to the emergence of intense slip bands, which cause local concentrations of stresses if blocked at grain boundaries and are the cause of microcrack nucleation. The crack propagation direction locally diverged from the plane of the operation of maximum normal stresses, whereas crack length increment was stepwise, which was most probably a result of the blockage at grain boundaries. In specimens loaded with a bending moment causing nominal stresses σ_{bna} = 80MPa in transverse section, the destruction of which took place after N_f=2.01-2.08·10^5 cycles, first cracks of the lengths of 80-100 μm were noticed after N_i=5.0·10^3 cycles of load changes, that is, after N_i=(0.024-0.025)N_f. When analyzing the propagation of fatigue cracks at the nominal stress σ_{bna} = 80MPa ≈ 0.24 $R_{0.2}$, the effect of macroscopic plastic strain ($\alpha_\varepsilon \approx 1.063 \cdot \alpha_\sigma$) may by ignored.

Increasing stress to σ_{bna} = 90MPa ≈ $0.27R_{0.2}$ causes a slight increase in strain concentration. The destruction of the specimens took place after N_f=1.60-1.80·10^5. No significant changes in the propagation of fatigue cracks were observed in the specimens.

At σ_{bna}=100MPa, on the surfaces of tested specimens, there were observed microscopic signs of the presence of plastic strains, which was confirmed by the performed numerical analysis, by which the values of the factors of stress concentration and deformation were obtained and they were $\alpha_\varepsilon \approx 1.111 \cdot \alpha_\sigma$. The fatigue life of the specimens was N_f=1.40-1.50·10^5 cycles. However, there was observed a significantly smaller, in comparison with specimens tested at lower nominal stresses, increment in crack length during the first 5000 load change cycles. Crack lengths measured at particular stress levels may be expressed by the following relation: l_{100}:l_{90}:l_{80}=1:1.335:1.210. An unusual fatigue crack development observed in specimens tested at σ_{bna}=100MPa is caused by the presence of intense plastic strains in the vicinity of the notch bottom. The strains, which appear already during the initial load cycles, cause the emergence of a reinforced zone, which causes a slight decrease in crack growth rate within that zone. Still, the aforementioned phenomenon does not produce a measurable benefit in the form of extending the fatigue life of the specimen. Crack propagation through the reinforced zone results in crack length increment, so that the abovementioned relation becomes l_{100}:l_{90}:l_{80}=1:0.966:0.870 after 1000 load change cycles.

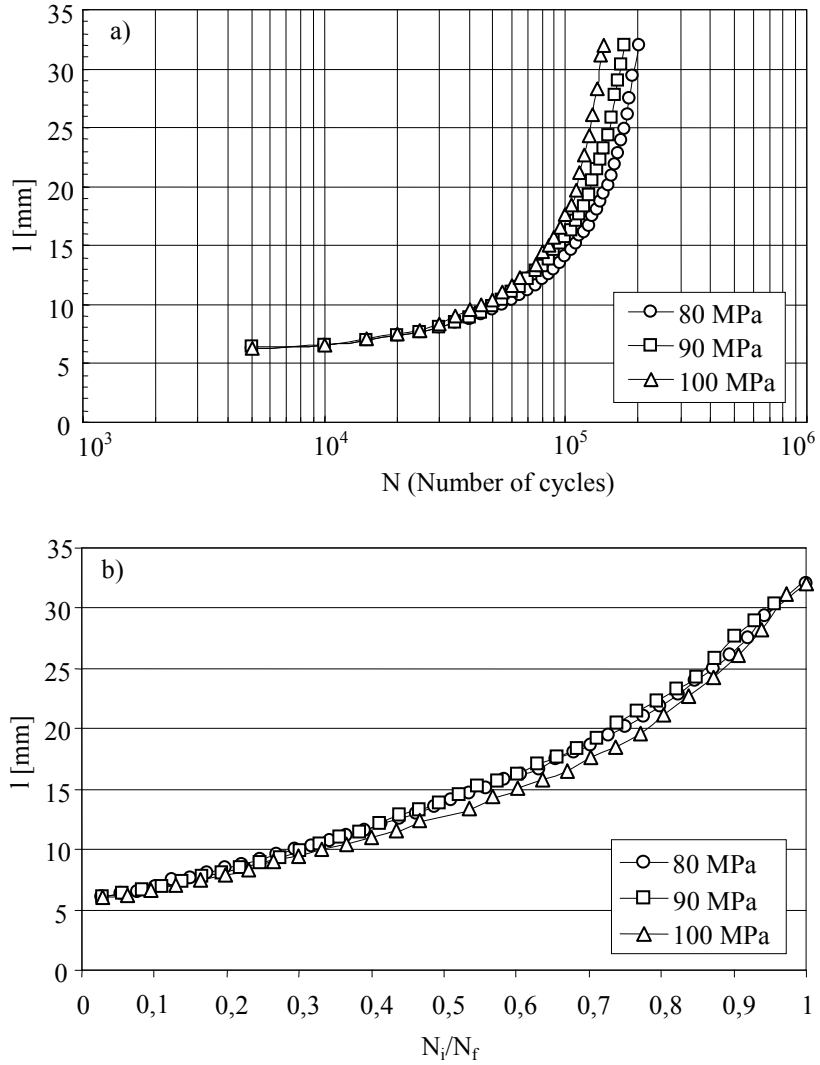

Fig. 9. Crack growth in a D16 alloy specimen at σ_{bna} = 80, 90 and 100MPa. Crack lengths depending on the number of load cycles N (a) and the ratio N_i/N_f (b)

4.2. Fatigue crack growth rate

The results of the measurements of crack lengths, l, for a particular number of cycles, N, constituted the basis for calculating and describing crack growth rates. Crack growth rates were calculated by formulas mentioned in point 4. Subsequently, the diagrams $dl/dN=f(N_i/N_f)$, and $dl/dN=f(\Delta J)$, where ΔJ is the J-integral range, were produced (see Fig. 10).

Regular crack growth observed during fatigue tests is reflected in the diagrams of crack growth rates in specimens. It is a feature of crack propagation which is decisively influenced by both the microstructure and mechanical properties of the tested alloy. It ought to be remembered that the optimum structure that provides the best fatigue properties depends also on the state of stresses which the material is subject to. For a plane state of stress, the best properties are obtained for recrystallized fine-grained structures. Whereas in the case of a plane state of strain, a non-recrystallized structure is preferable. The reason for that is that the fatigue cracking resistance in a plane state of stress can be controlled by the plastic strain size near the crack tip. Alloys of fine recrystallized grain structure attain maximum plastic strain near the crack tip. Whereas cracking resistance in a plane state of strain is influenced by particles that are present at grain boundaries. Moreover, higher cracking resistance of non-recrystallized materials results from a longer distance between boundaries in such materials.

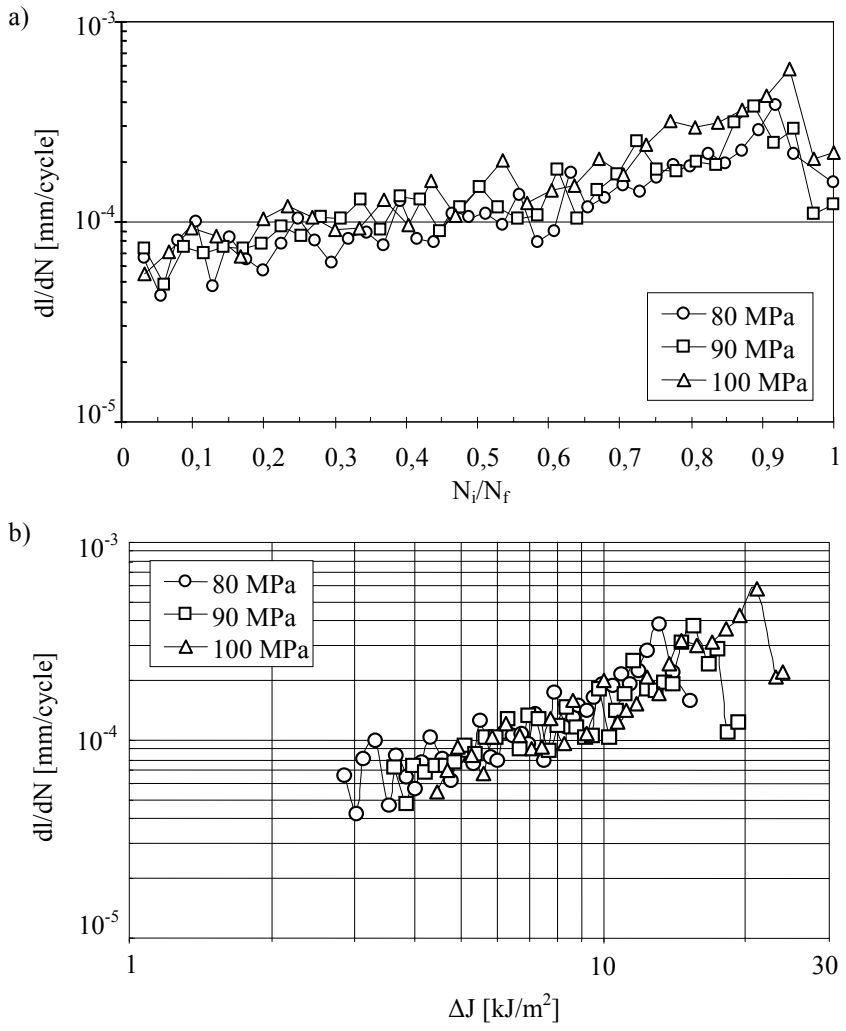

Figure 10. Crack growth rates in the D16 alloy specimens at σ_{bna} = 80, 90 and 100MPa depending on the ratio N_i/N_f (a) and the J-integral range (b)

5. MICROSTRUCTURES OF FATIGUE FRACTURE SURFACES

The mechanism of fatigue crack propagation was traced by means of examining microstructures of fracture surfaces with the TEM JEOL JEM 1230 microscope, using carbon-sprayed and platinum-shaded acetylcellulose replicas.

In the course of fatigue tests, cracks were always initiated at the bottom of the cut out notch, regardless the pre-stress level; the direction of propagation coincided with the plane of maximum normal stresses.

The micrographs obtained with the transmission electron microscope (TEM), delivered information on the mechanism of cracking in the specimens under tests. Some selected sections of fractures shown in Fig. 11 come from the specimens made of the D16 and tested at $\sigma_{bna} = 100$ MPa.

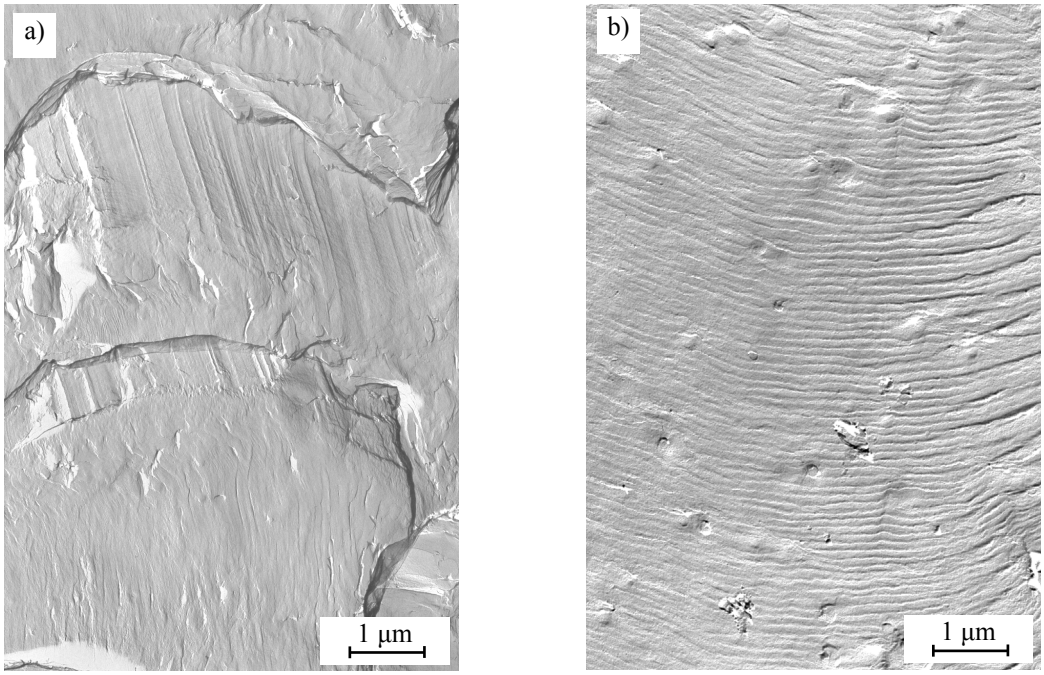

Fig. 11. Initiation (a) and fatigue (b) areas of crack growth in specimens made of the D16 alloy at $\sigma_{bna} = 100$ MPa

Within the notch, in the area of stress and strains concentrations, there are microareas that differ from typical fatigue fractures and well illustrate the mechanism of quick fatigue failing of the material (Figs 11a). What is meant is the rapidity of changes taking place and of the process of cracking. It is manifested with a complex microstructure of a fracture in a specimen made of the D16 alloy, with local shearing of surface bands and numerous fracture-induced fissures. Fig. 11a shows jogs that prove a crack to snap through between planes of growth of many microcracks which propagate in adjacent layers of the strongly deformed structure of the alloy under examination. The jogs have been created due to the shearing or breaking of bridges which separate planes of cracking from each other.

The fracture microstructure changes in the fatigue area. At the distance of approximately 0.4mm from the bottom of the notch, a band of plastic and irregular fatigue striations appears (Figs 11b). Visible differences in interstriation distances at the same depth prove local changes in cracking rates.

6. DETERMINISTIC DESCRIPTION OF THE CRACKING

The in the paper presented model has been based on some description of the cracking, with J integral in the form of (3). There are two empirical coefficients used in the above-shown formula. From the standpoint of the model being formulated, specific values are of no or little importance. Their remaining independent of the current length of the crack is what actually matters. Predicted is estimation - on the grounds of experimental findings - of quantities indispensable in the model, with no need to give, e.g. values of stress. Hence, all the below introduced dependences can also be used for, e.g. the range of effective stress.

The following formula has been accepted to describe the rate of cracking:

$$\frac{dl}{dN} = c\left(J_{\max}\right)^m \tag{4}$$

where: N – the number of loading cycles,
c, m – constants.

The following relationship has been assumed to relate strains and stresses:

$$\varepsilon_{\max} = a\sigma_{\max} \tag{5}$$

where: a - factor of proportionality, further on assumed to remain constant.

Due to transformations, the J integral takes the following form:

$$J_{max} = \left[\frac{1{,}24}{E} + 1{,}02\frac{a}{\sqrt{n'}}\right]\left(\sigma_{max}\right)^2 l \tag{6}$$

Having substituted (6) for J_{max} in (4), the following is arrived at:

$$\frac{dl}{dN} = c\left[\frac{1{,}24}{E} + 1{,}02\frac{a}{\sqrt{n'}}\right]^m \left(\sigma_{max}\right)^{2m} l^m \tag{7}$$

Using the following notification:

$$A = c\left[\frac{1{,}24}{E} + 1{,}02\frac{a}{\sqrt{n'}}\right]^m \left(\sigma_{max}\right)^{2m} \tag{8}$$

we get:

$$\frac{dl}{dN} = Al^m \tag{9}$$

While setting to solve this equation, one has to take account of the value of the m exponent.

I. For $m = 1$:

$$\int \frac{dl}{l} = \int A dN$$

$$\ln l = AN$$

Allowing for the condition that the initial crack length $l(N = 0) = l_0$, we get:

$$l = l_0 e^{AN} \tag{10}$$

II. For $m \neq 1$:

$$\int \frac{dl}{l^m} = \int A dN$$

$$\frac{1}{1-m} l^{1-m} = AN$$

Allowing for the initial condition:

$$l = \left[(1-m)AN + l_0^{1-m}\right]^{\frac{1}{1-m}}$$

Taking account of that the exponent m of value greater than unity, the above relationship can be written down in the following form:

$$l = \frac{l_0}{\left[1-(m-1)ANl_0^{m-1}\right]^{\frac{1}{m-1}}} \tag{11}$$

Therefore, the current length of the crack l is described with the following equation:

$$l = \begin{cases} l_0 e^{AN} & ; m = 1 \\ \dfrac{l_0}{\left[1-(m-1)ANl_0^{m-1}\right]^{\frac{1}{m-1}}} & ; m \neq 1 \end{cases} \tag{12}$$

It might prove useful to check whether the solution of the above equation remains continuous towards the value of the exponent m. Left- and right-hand limits of the function $l(m)$ at the point $m = 1$ are equal to each other ($g_l = g_p = g$). A value of this g limit is:

$$g = \lim_{m \to 1} \frac{l_0}{\left[1-(m-1)ANl_0^{m-1}\right]^{\frac{1}{m-1}}}$$

Expression in the denominator gives an indeterminate symbol of the type 1^{∞}. To make use of the de l'Hospital theorem, we have applied a transformation $u^v = e^{v \ln u}$

$$g = \frac{l_0}{\lim\limits_{m\to 1}\left[1-(m-1)ANl_0^{m-1}\right]^{\frac{1}{m-1}}} = {}^{1^{\infty}}\frac{l_0}{\lim\limits_{m\to 1} e^{\frac{1}{m-1}ln\left[1-(m-1)ANl_0^{m-1}\right]}} = \frac{l_0}{e^{\lim\limits_{m\to 1}\frac{1}{m-1}ln\left[1-(m-1)ANl_0^{m-1}\right]}}$$

$$g \underset{H}{=} \frac{l_0}{e^{\lim\limits_{m\to 1}\frac{\frac{-ANl_0^{m-1}-(m-1)ANl_0^{m-1}\ln l_0}{1-(m-1)ANl_0^{m-1}}}{1}}} = \frac{l_0}{e^{\lim\limits_{m\to 1}\frac{-ANl_0^{m-1}-(m-1)ANl_0^{m-1}\ln l_0}{1-(m-1)ANl_0^{m-1}}}} = \frac{l_0}{e^{\frac{-AN}{1}}} = \frac{l_0}{e^{-AN}} = l_0 e^{AN}$$

The calculated limit of function equals its value at the point $m = 1$; hence, the solution given with eq (12) remains continuous towards the exponent m, and two ranges of applicability of this solution result only from the limitations of the mathematical notation.

The checkup of the correctness of the solution found:

I. For $m = 1$:

$$\frac{dl}{dN} = l_0 A e^{AN} = Al$$

Having compared the above expression to the formula (9) for $m = 1$, one can easily find that the solution is correct.

II. For $m \neq 1$:

$$\frac{dl}{dN} = \frac{-l_0\frac{1}{m-1}\left[1-(m-1)ANl_0^{m-1}\right]^{\frac{1}{m-1}-1}(-1)(m-1)Al_0^{m-1}}{\left[1-(m-1)ANl_0^{m-1}\right]^{\frac{2}{m-1}}} = \frac{\left[1-(m-1)ANl_0^{m-1}\right]^{\frac{2-m}{m-1}}Al_0^m}{\left[1-(m-1)ANl_0^{m-1}\right]^{\frac{2}{m-1}}} =$$

$$= \frac{Al_0^m}{\left[1-(m-1)ANl_0^{m-1}\right]^{\frac{m}{m-1}}} = A\left[\frac{l_0}{\left[1-(m-1)ANl_0^{m-1}\right]^{\frac{1}{m-1}}}\right]^m = Al^m$$

Again, having compared the above expression to the formula (9) for $m \neq 1$, one can easily find that the solution is correct.

7. PROBABILISTIC DESCRIPTION OF THE CRACKING

What has been assumed while setting to formulate a probabilistic model is as follows:

1. Loading cycles of Δt duration may occur rather randomly, at the rate λ i.e. $\lambda\Delta t \leq 1$, than continuously.
2. Consideration is given to such lengths of fatigue cracks that for some interval (or for a certain number of loading cycles) the probability that a catastrophic fracture occurs in a structural member equals zero.
3. The rates of fatigue cracking are described in the deterministic approach with the above-presented relationships.

On such assumptions the following difference equation can be written down, one that describes the crack growth dynamics in probabilistic terms:

$$U_{l,t+\Delta t} = (1-\lambda\Delta t)U_{l,t} + \lambda\Delta t U_{l-\Delta l,t} \tag{13}$$

where: $U_{l,t}$ – probability that at time instant t the crack length is l.

After transition to functional notation, the following can be written down:

$$U(l,t+\Delta t) = (1-\lambda\Delta t)U(l,t) + \lambda\Delta t U(l-\Delta l,t) \tag{14}$$

where: $U(l,t)$ – density function of crack lengths.

The above shown crack length increment during one cycle Δl will be found from the relationships of the deterministic model.

With eq (9) applied, after transition to the determination of increments for one loading cycle($\Delta N = 1$), and after having allowed for $N = \lambda t$, here is what resulted:

$$\Delta l = \alpha l^m$$

What comes out, after account taken of the expression (8) that defines the crack length, is:

$$\Delta l = \begin{cases} \alpha l_0 e^{\alpha\lambda t} & ; m = 1 \\ \dfrac{\alpha l_0^m}{\left[1-(m-1)\alpha\lambda t l_0^{m-1}\right]^{\frac{m}{m-1}}} & ; m \neq 1 \end{cases} \tag{15}$$

The α coefficient introduced at this point is of a little bit different sense than the A used earlier. And so, the α coefficient takes account of the probability P_{th} that in case a loading cycle occurs, the stress $(\sigma_{max})^{2m}$ will exceed some threshold value and the crack growth will result.

$$\alpha = c\left[\frac{1{,}24}{E} + 1{,}02\frac{a}{\sqrt{n'}}\right]^m P_{th}(\sigma_{max})^{2m} \tag{16}$$

To arrive at a differential equation, terms of eq (10) need to be subjected to series expansion, with reduction to several terms of expansion:

$$U(l,t+\Delta t) \approx U(l,t) + \frac{\partial U(l,t)}{\partial t}\Delta t$$

$$U(l-\Delta l,t) \approx U(l,t) - \frac{\partial U(l,t)}{\partial l}\Delta l + \frac{1}{2}\frac{\partial^2 U(l,t)}{\partial l^2}\Delta l^2$$

After both substitution of terms of eq (10) by these dependences, and allowing for the expression to determine the crack length increment Δl, the following has been reached:

$$U(l,t)+\frac{\partial U(l,t)}{\partial t}\Delta t=(1-\lambda\Delta t)U(l,t)+\lambda\Delta t\left[U(l,t)-\frac{\partial U(l,t)}{\partial l}\Delta l+\frac{1}{2}\frac{\partial^2 U(l,t)}{\partial l^2}\Delta l^2\right]$$

$$\frac{\partial U(l,t)}{\partial t}=-\dot{b}(t)\frac{\partial U(l,t)}{\partial l}+\frac{1}{2}\dot{w}(t)\frac{\partial^2 U(l,t)}{\partial l^2} \tag{17}$$

where:

$$\dot{b}(t)=\lambda\Delta l=\begin{cases}\lambda\alpha l_0 e^{\alpha\lambda t} & ;m=1\\ \dfrac{\lambda\alpha l_0^m}{\left[1-(m-1)\alpha\lambda t l_0^{m-1}\right]^{\frac{m}{m-1}}} & ;m\neq 1\end{cases}$$

$$\dot{w}(t)=\lambda\Delta l^2=\begin{cases}\lambda\alpha^2 l_0^2 e^{2\alpha\lambda t} & ;m=1\\ \dfrac{\lambda\alpha^2 l_0^{2m}}{\left[1-(m-1)\alpha\lambda t l_0^{m-1}\right]^{\frac{2m}{m-1}}} & ;m\neq 1\end{cases}$$

In the next step, a solution to eq (13) should be found in the form of the Dirac equation such as to get the function integral equals unity.

The solution looked for shows the form of the Gaussian distribution:

$$U(l,t)=\frac{1}{\sqrt{2\pi w(t)}}e^{-\frac{(l-b(t))^2}{2w(t)}} \tag{18}$$

In the above formula, *b(t)* stands for the expected value of the crack length, whereas *w(t)* – variance of crack length distribution.

I. For $m = 1$:

$$b(t)=l_0 e^{\alpha\lambda t}$$

$$w(t)=\frac{\alpha l_0^2}{2}\left(e^{2\alpha\lambda t}-1\right)$$

II. For $m \neq 1$:

$$b(t)=\frac{l_0}{\left[1-(m-1)\alpha\lambda t l_0^{m-1}\right]^{\frac{1}{m-1}}}$$

$$w(t)=\frac{\alpha l_0^{m+1}}{m+1}\left[\frac{1}{\left[1-(m-1)\alpha\lambda t l_0^{m-1}\right]^{\frac{m+1}{m-1}}}-1\right]$$

8. ESTIMATION OF PARAMETERS OF DISTRIBUTION

Determination of parameters of distribution (14) needs evaluation of the coefficient α and exponent m.

To estimate parameters of distribution, the maximum likelihood and the least squares methods were used (descriptions of both methods have been neglected, since they remain in common use). Let us assume that we've got service- or lab-tests originated data on crack propagation. The data is in the following form:

$$[(l_0, t_0), (l_1, t_1), ..., (l_n, t_n)] \tag{19}$$

I. Estimation of the coefficient α

From the logarithm of the likelihood function, after having differentiated against the parameter of interest and after transition to functional notation, the following equations have been arrived at:

$$\begin{cases} \sum_{k=0}^{n-1}\left(l_{k+1}-l_k\right) = l_0\sum_{k=0}^{n-1}\left(e^{\alpha\lambda t_{k+1}} - e^{\alpha\lambda t_k}\right); & m=1 \\ \sum_{k=0}^{n-1}\left(l_{k+1}-l_k\right) = l_0\sum_{k=0}^{n-1}\left(\frac{1}{\left[1-(m-1)\alpha\lambda t_{k+1}l_0^{m-1}\right]^{\frac{1}{m-1}}} - \frac{1}{\left[1-(m-1)\alpha\lambda t_k l_0^{m-1}\right]^{\frac{1}{m-1}}}\right); & m\neq 1 \end{cases} \tag{20}$$

and after transformation thereof:

$$\begin{cases} l_n = l_0 e^{\alpha\lambda t_n}; & m=1 \\ l_n = l_0\dfrac{1}{\left[1-(m-1)\alpha\lambda t_n l_0^{m-1}\right]^{\frac{1}{m-1}}}; & m\neq 1 \end{cases} \tag{21}$$

Having solved the above equations vs α, the following is found:

$$\begin{cases} \alpha = \dfrac{1}{\lambda t_n} ln\dfrac{l_n}{l_0}; & m=1 \\ \alpha = \dfrac{1-\left(\dfrac{l_0}{l_n}\right)^{m-1}}{(m-1)\lambda t_n l_0^{m-1}}; & m\neq 1 \end{cases} \tag{22}$$

The dependences found make estimation of value of the coefficient α possible for some known value of the exponent m.

II. Estimation of the exponent *m*

With the least squares method applied, the following relationship has been found:

$$\sum_{k=0}^{n}(l_k - B_k)C_k = 0 \tag{23}$$

where:

$$C_k = \frac{B_k}{1-m}\left[ln\frac{B_k}{l_0} - \frac{\lambda t_k}{\lambda t_n}\left(\frac{l_n}{B_k}\right)^{1-m} ln\frac{l_n}{l_0}\right] \tag{24}$$

$$B_k = l_0\left\{1 - \frac{\lambda t_k}{\lambda t_n}\left[1 - \left(\frac{l_n}{l_0}\right)^{1-m}\right]\right\}^{\frac{1}{1-m}} \tag{25}$$

The result has taken some confounded form. It is considerably difficult to find the analytical form of the estimator *m*. While verifying the computational model, it was decided to numerically solve eq (19) with the method of bisection.

Estimation of necessary coefficients that occur in the resultant probability distribution resolves itself into the following steps:

1. Assuming the value of the exponent $m = 1$, or estimation thereof according to (19);
2. Estimation of the value of the coefficient α according to (18), in compliance with the value of *m*.

9. FATIGUE LIFE OF A MEMBER

Using the probability distribution with known parameters one can set about estimating fatigue life of a given member.

Therefore, one should determine the probability *R(t)* that the assumed, acceptable crack length l_d is not exceeded. This should take the following form:

$$\boldsymbol{R(t) = P(l \le l_d) = \int_{-\infty}^{l_d} U(l,t)dl} \tag{26}$$

The probability *R(t)* can be treated as the reliability of a given member in terms of fatigue cracking. It would be convenient to use tables of Gaussian distribution to determine the *R(t)*. No doubt, the operation needs standardization of random variables. With some specific change in reliability with time, for the assumed minimum level of reliability R^*, one can determine fatigue life of the member *T* from the following condition:

$$R(t) \ge R^* \tag{27}$$

Computations are to be carried out for subsequent values of *t*, for which condition (25) is satisfied. The greatest value $t = T$ that satisfies condition (23) is the estimate of the member's life.

10. EXPERIMENTAL VERIFICATION OF THE COMPUTATIONAL MODEL

Dependences derived throughout sections 6 ÷ 9 gave grounds for the probabilistic description of crack propagation and the estimation of life of the specimens under tests. Plots that illustrate measurements of crack lengths and the courses of the expected values of crack lengths b(t) for some selected specimen tested at σ_{bna} = 100MPa has been presented in Fig. 12.

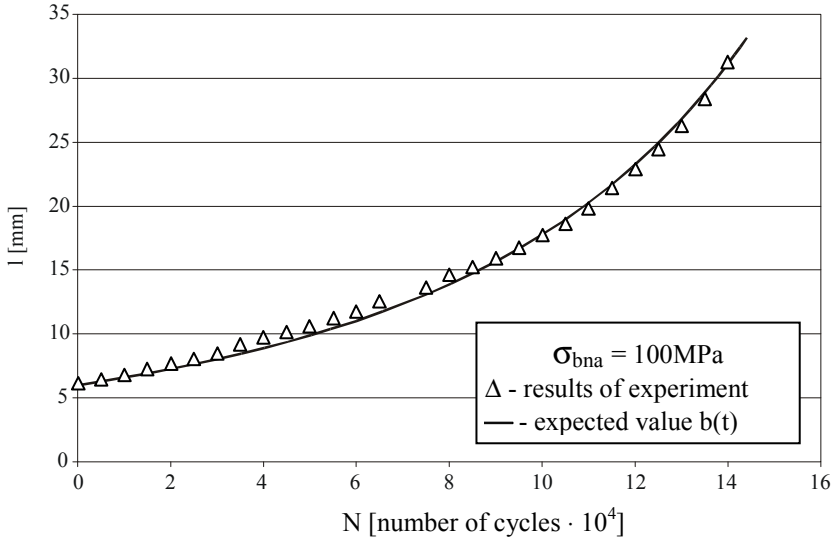

Fig. 12. Recorded and predicted crack lengths in the specimen tested at σ_{bna} = 100MPa

While calculating fatigue life, assumed were: the initial crack length $l_0 = 6$ [mm] and the acceptable crack length $l_d = 32$ [mm], both resulting from geometric dimensions of the specimens used in fatigue tests. The assumed minimum reliability level was $R^* = 0.9$ [-].

Fig. 13 show plot that illustrate the courses of probability *R(t)* for analyzed specimen tested at σ_{bna} = 100MPa .

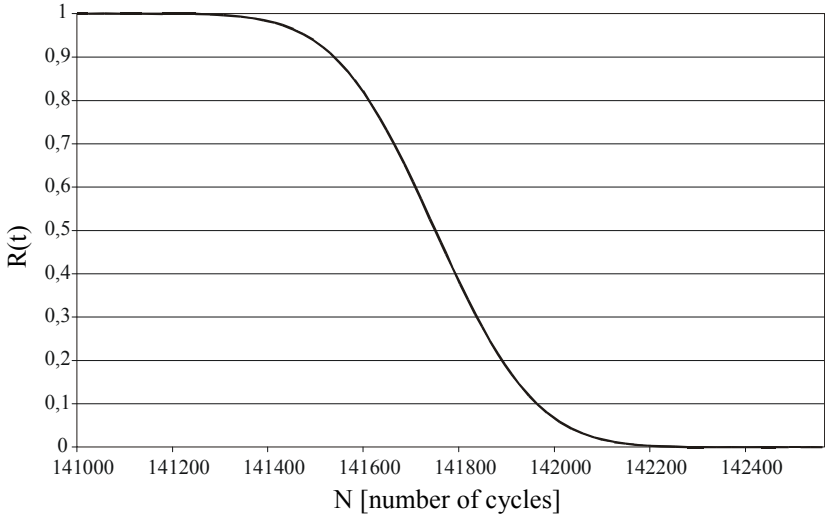

Fig. 13. Change in the probability R(t) that the acceptable crack length l_d in the specimen tested at σ_{bna} = 100MPa is exceeded

The calculated and experimentally found fatigue lives of all analyzed specimens have been shown in Fig. 14.

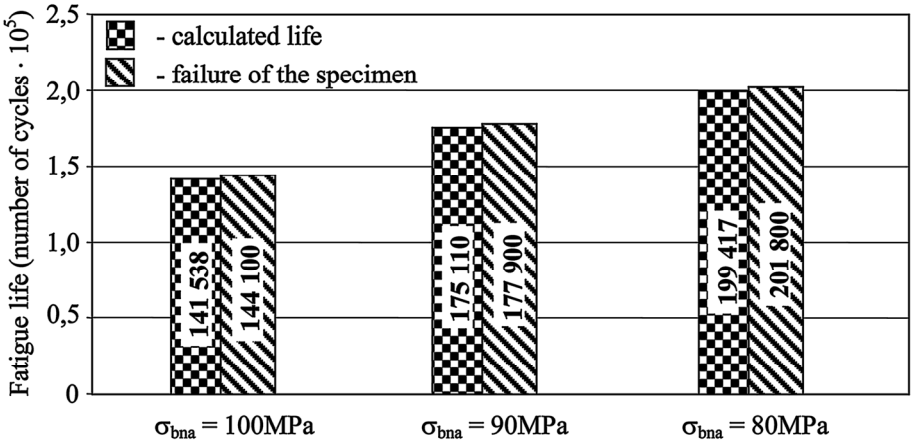

Fig. 14. Calculated and experimentally found fatigue lives of specimens made of the D16 alloy

11. SUMMARY

The paper discusses the research on the emergence and propagation of fatigue cracks in the D16 aluminium alloy, which is used in aircraft skins, with taking into consideration the notch in the form of a central hole with side cuts.

The effect of the notch geometry on the values of stress concentration and deformations as well as the range of the notch action were determined by means of the finite elements method using a three-dimensional geometric model of the specimen with a central fissure. The results of numerical calculations made it possible to analyze the effect of the notch on the recorded emergence and growth of fatigue cracks in tested alloys. The values of the factors of stress concentration and deformations in the area of the notch bottom were calculated on the basis of the analysis results.

The emergence and growth of cracks were analyzed under the conditions of flat bending at σ_{bna}=80, 90 and 100 MPa. Crack initiation took place at the notch bottom in slip bands located in the matrix of the tested alloy. The mechanism of crack development was investigated on the basis of the images of the microstructure of crack surfaces taken by means of the transmission microscope (TEM). The microstructure of crack surfaces showed a complex cracking mechanism both at the initial stage of crack growth in the notch-affected zone and beyond that zone.

The in the paper suggested probabilistic model provides capability to forecast fatigue lives of structural members. What is needed for the model is the knowledge of the service-induced crack growth, which comprises full probabilistic description of crack propagation, and therefore is the source of information on stochastic factor of the cracking. Data indispensable for computations have been collected in the course of experimental work on fatigue crack growth and propagation in model members made of aluminium alloy D16.

The recorded (during experimental work) and expected crack lengths in the specimens under examination have shown satisfactory compatibility. Safe estimate of life has been found. The computed lives of specimens expressed with the number of loading cycles to failure are lower and differ by 1.2 – 2.4 % from those found experimentally.

12. REFERENCES

[1] Peterson, R. (1974). *Stress concetration factors*. New York: Wiley.

[2] Hertzberg, R. W. (1983). *Deformation and Fracture Mechanics of Engineering Materials* (2nd ed.). New York/Chichester/Brisbane/Toronto/Singapore: John Wiley & Sons.

[3] Pilkey, W. (1997). *Peterson's stress concentration factors* (2nd ed.). New York: John Wiley & Sons.

[4] Pluvinage, G., & Gjonaj, M. (2000). Notch Effects in Fatigue and Fracture. *NATO Science Series II: Mathematics, Physics and Chemistry,* 11. Dordrecht/Boston/London: Kluwer Academic Publishers.

[5] Andrews, E. W., & Gibson, L. J. (2001). The influence of cracks, notches and holes on the tensile strength of cellular solids. *Acta Materialia,* 49, 2975-2979.

[6] Strandberg, M. (2002). Fracture at V-notches with contained plasticity. *Engineering Fracture Mechanics,* 69, 403-415.

[7] Troyani, N., Hernandez, S. I., Villarroel, G., Polonais, Y., & Gomes, C. (2004). Theoretical stress concentration factors for short flat bars with opposite U-shaped notches subjected to in-plane bending. *International Journal of Fatigue*, 26, 1303-1310.

[8] Tlilan, H. M., Yousuke S., & Tamotsu, M. (2005). Effect of notch depth on strain-concentration factor of notched cylindrical bars under static tension. *European Journal of Mechanics A/Solids.* 24, 406-416.

[9] Spencer, K., Corbin, S. F., & Lloyd, D. J. (2002). Notch fracture behaviour of 5754 automotive aluminium alloys. *Materials Science & Engineering.* A 332, 81-90.

[10] Tokaji, K. (2005). Notch fatigue behaviour in a Sb-modified permanent-mold cast A356-T6 aluminium alloy. *Materials Science & Engineering*. A 396, 333-340.

[11] Caleyo, F., Gonzalez, J. L., & Hallen, J. M. (2002). A study on the reliability assessment methodology for pipelines with active corrosion defects. *International Journal of Pressure Vessels and Piping.* 79, 77-86.

[12] Ahammed, M. (1998). Probabilistic estimation of remaining life of a pipeline in the presence of active corrosion defects. *International Journal of Pressure Vessels and Piping* 75, 321-329.

[13] Ahammed, M. (1997). Prediction of remaining strength of corroded pressurized pipelines. *International Journal of Pressure Vessels and Piping*. 71, 213-217.

[14] Ahammed, M., & Melchers, R. E. (1997). Probabilistic analysis of underground pipelines subject to combined stress and corrosion. *Engineering Structures*, 19(12), 988-994.

[15] Kocańda, D., Kocańda, S., Miller, K. J., & Tomaszek, H. (1999). Experimental and theoretical investigations of short fatigue crack growth in laser hardened medium carbon steel. *Engineering Against Fatigue* (pp. 501-507). Rotterdam-Brookfield: A.A. Balkema.

[16] Kocańda, D., Kocańda, S., & Tomaszek, H. (1999). Probabilistic approach to the short and long fatigue crack growth description in a notched member, In Fatigue'99: International Fatigue Congress, Beijing, 4/1999, (pp. 2673-2678), China, Cradley Heath: EMAS, Higher Education Press Beijing.

[17] American Society for Testing and Materials. (1976). Dowling N. E. & Begley J. A. (Eds.). In Mechanics of crack growth. ASTM STP 590, pp. 82-103. West Conshonocken, PA: ASTM International.